



Extreme drought conditions increase variability of nitrate through a stream network, with limited influence on the spatial patterns of stream phosphate

Dana R. Warren · Julie C. Pett-Ridge · Catalina Segura · Matthew J. Kaylor · Emily D. Heaston

Received: 16 November 2021 / Accepted: 26 June 2022
© The Author(s), under exclusive licence to Springer Nature Switzerland AG 2022

Abstract Nutrient availability is an important control on ecosystem processes in streams. In this study, we explored how an extreme summer drought affected spatial patterns of nutrient availability along a fourth-order stream network in western Oregon. Droughts are expected to become increasingly common and more severe across western North America and around the world. Understanding how nutrient availability changes locally and throughout a stream network during low-flow periods provides important insight into drought impacts on stream ecosystems.

We quantified nitrate (NO_3^-) and phosphate (PO_4^{3-}) concentrations every 50 m along 11.5 km of a headwater stream network during three summer periods of different drought intensity that encompassed some of the lowest discharges observed in this system over its 70-year hydrologic record. Semi-variogram analysis indicated that concentrations of the dominant limiting nutrient, NO_3^- , became increasingly spatially heterogeneous during the most extreme drought conditions, whereas spatial variability of PO_4^{3-} concentrations remained similar across all three flows. Synoptic sampling during the most severe low-flow period revealed hotspots of biogeochemical processing that would be missed if sampling were conducted during higher flows when surface water dilution and more rapid transport of limiting nutrients would dampen local signals. Along a 3 km section of the upper mainstem, an increase in N availability during the drought led to a reduction in the degree of N-limitation and a potential shift toward P-limitation. Our results suggest that projected climate-induced changes in hydrology in this region will modify local nutrient availability.

Responsible Editor: Jennifer Leah Tank

Supplementary Information The online version contains supplementary material available at <https://doi.org/10.1007/s10533-022-00953-5>.

D. R. Warren (✉) · E. D. Heaston
Department of Forest Ecosystems and Society, Oregon State University, Richardson Hall, Corvallis, OR, USA
e-mail: dana.warren@oregonstate.edu

D. R. Warren · M. J. Kaylor
Department of Fisheries, Wildlife, and Conservation Sciences, Oregon State University, Corvallis, OR, USA

J. C. Pett-Ridge
Department of Crop and Soil Sciences, Oregon State University, Corvallis, OR, USA

C. Segura
Department of Forest Engineering, Resources and Management, Oregon State University, Corvallis, OR, USA

Keywords Nitrogen · Phosphorous · Stream network · Semi-variance analysis · Drought · Stream spatial patterns · H.J. Andrews

Introduction

In lotic ecosystems, discharge is a fundamental driver of nutrient supply, demand, and biogeochemical processing, which can in turn influence nutrient retention and flux within a stream network (Gomez-Gener et al. 2020; Peterson et al. 2001; Wollheim et al. 2018). Changing climate conditions are expected to alter stream discharge patterns across western North America and in many other regions around the world by creating more and longer periods of extreme low flow conditions (droughts) (IPCC 2021; Mote et al. 2016). As flow decreases through a prolonged drought, the relative influence of localized nutrient inputs and hotspots of biogeochemical processing may each become more pronounced, resulting in greater spatial variability of nutrient availability along a stream with implications for spatial variability of nutrient limited ecosystem processes. In some regions drought may occur as a result of reduced rainfall, while in other regions total precipitation may remain unchanged, but changes in the timing and type of precipitation will lead to drought (Sheffield and Wood 2008; Van Loon et al. 2016). In regions where summer flows are reliant upon winter snowpack, a shift toward more precipitation falling as rain rather than snow will result in reduced snowpack, earlier onset of spring snowmelt, and decreased summer flows (Leibowitz et al. 2014; Sproles et al. 2013). In the western US, one such low-snowpack year occurred in 2015, leading to extremely low early- and mid-summer discharge in streams across Washington, Oregon, and California (Mote et al. 2016; Segura 2021; Ward et al. 2020).

A number of studies have assessed the effects of drought on nutrient concentrations at select locations or on nutrient fluxes from small watersheds within a network (Davis et al. 2014; Kane et al. 2008; Mast et al. 2014), and other studies have evaluated spatial patterns of stream nutrient concentration throughout a network during a single time period (Bernal et al. 2015; Dong et al. 2017; Likens and Buso 2006; McGuire et al. 2014; Zimmer et al. 2013). Fewer studies have integrated spatial and temporal sampling in evaluating the impacts of drought on the spatial patterns of nutrient concentrations throughout a stream network (Dent and Grimm 1999; Hur et al. 2007). Assessing the spatial patterns of stream nutrients during extreme low-flow events (drought) can provide

information about potential patchiness of stream productivity. For example, working in a desert stream through a period of benthic biofilm succession that also encompassed a severe reduction in stream discharge (such that large sections of the stream became disconnected), Dent and Grimm (1999) evaluated changes in the spatial pattern of nutrients and found that spatial heterogeneity of the limiting nutrient (nitrogen) increased with time since the flood event. They attribute this heterogeneity to a combination of shifts in demand associated with changing algal communities and localized areas of high input relative to surface discharge. This pattern has not been widely assessed outside of a desert landscape or at a high spatial resolution that may more clearly capture localized patterns in stream nutrient dynamics.

The two most commonly limiting nutrients for aquatic primary producers and stream heterotrophs are nitrogen (N) and phosphorous (P) (Capps et al. 2011; Hill and Knight 1988; Tank and Dodds 2003). In most ecosystems, the inorganic soluble forms of N [nitrate (NO_3^-) and ammonium (NH_4^+)] and P (phosphate (PO_4^{-3})) are the most bioavailable. Streams often have distinctly different degrees of background availability of inorganic N or P, leading to differences in which element is likely to be limiting for biological processes (Tank and Dodds 2003). In relatively unaltered systems, available inorganic N is primarily biologically derived, and in systems like the Oregon Cascades where N is frequently a limiting nutrient for primary production and decomposition in streams (Aumen et al. 1983; Cairns and Lajtha 2005; Warren et al. 2017), cycling of N is strongly influenced by biotic processes. In forested systems in the western US with limited anthropogenic nutrient input, inorganic N in streams is often derived from trees with N-fixing symbionts in the upland catchment slopes as well as along stream riparian zones, which can generate net nitrification and subsequent nitrate leaching to groundwater which flows into streams (Cairns and Lajtha 2005; Compton et al. 2003). In contrast to N, P in these systems is derived primarily from an abiotic process (rock weathering), which occurs more uniformly throughout catchments than N fixation. Phosphorus has not been shown to strongly limit to stream biofilms in Pacific Northwest headwater stream systems (Hill and Knight 1988; Warren et al. 2017).

This study examines spatial patterns of NO_3^- -N and PO_4^{-3} -P concentrations in a forested temperate

fourth-order watershed in the western Cascade Mountains in Oregon. We quantified stream nutrient concentrations every 50 m along 11.5 km of the stream network over three summer periods with different drought conditions, including an extreme drought in late summer 2015. In addition to assessing spatial and temporal trends in nutrient concentrations, we compared NO_3^- -N and PO_4^{3-} -P patterns to the spatial patterns of chloride (Cl^-), which is sourced from sea salt aerosols in atmospheric inputs and is assumed to be a conservative and non-reactive in streams (Stream-Solute-Workshop 1990), providing a tracer of hydrologic inputs and simple dilution as well as potential evaporative concentration of stream water during drought. We focus specifically on how the severe drought conditions in summer 2015 affected the spatial and temporal patterns of stream nutrient availability in a headwater network. Given potentially high biological demand for N in these systems leading to areas of increased uptake, and given the increased importance of local groundwater input processes under low flow conditions (Segura et al. 2019), we expected spatial variability of inorganic N availability to increase during the 2015 drought. Further, given that P has not been widely documented as a limiting nutrient for primary production in Cascade Mountain streams, and the relatively easily weathered volcanic bedrock that dominates that Cascade Mountains, we expected inorganic P availability to be less variable than inorganic N availability throughout the network and over a range of stream drought conditions.

Methods

Study site and field methods

This study was conducted along 11.5 km of the stream network of McRae Creek, a fourth-order 16 km² tributary to Lookout Creek in the H. J. Andrews Experimental Forest (Fig. 1) located in the central Cascade Mountains of western Oregon. This region has a Mediterranean climate with cool wet winters and hot dry summers, with more than 80% of total precipitation falling between November and May. The McRae Creek basin has snow throughout most winters at the highest elevations, and spring and early summer flows are strongly affected by snowmelt and snowpack depth. Given the absence of summer

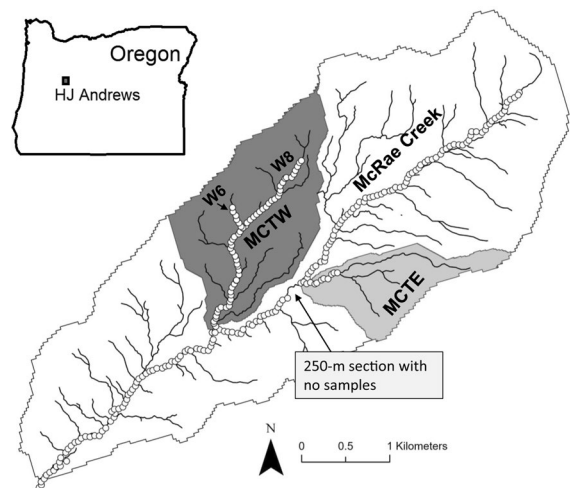


Fig. 1 Map of the McRae Creek stream network located in the HJ Andrews Experimental forest in the western Cascade Mountains of central Oregon. Dots represent sampling locations and collectively encompass ~11.5 km of stream ranging from the fourth-order mainstem at its confluence with Lookout Creek up to first-order headwaters

precipitation this system experiences the lowest flows between August and September.

The McRae Creek basin is dominated by old-growth Douglas fir forests >450 years of age, however, there are a number of small patch clearcuts that were implemented in the 1970's and 1980's that occur within the old-growth matrix, and many of these cuts extend down to and across streams (Kaylor et al. 2017). Riparian forests are a mix of Douglas fir (*Pseudotsuga menziesii*), western hemlock (*Tsuga heterophylla*), western red cedar (*Thuja plicata*), big leaf maple (*Acer macrophyllum*), and red alder (*Alnus rubra*), with red alder typically more common in previously harvested riparian forests compared to late succession riparian forests (Kaylor and Warren 2017). The McRae Creek basin is underlain by Miocene andesitic tuff and tuff breccia (Swanson and Jones 2002). All of the survey areas in the tributaries and in the middle and lower parts of the mainstem are all on the ashflow tuff from the Sardine formation. The upstream section of the mainstem transitions to Sardine formation andesitic lava flows and pyroclastic flows (Bywater-Reyes et al. 2017). In this wet steep terrain runoff generally increases with drainage area. Although we did not measure stream-flow, we assumed as in previous efforts (Segura et al.,

2019), that McRae Creek system is a gaining stream network.

Nutrients were sampled during three separate campaigns encompassing different discharges and different phases in the annual hydrograph. The first sampling event was conducted over four days from June 29, 2015 to July 2, 2015. The second sampling event was conducted over three days from August 18, 2015 to August, 21 2015, and the third sampling event was conducted from June 27, 2016 to July 1, 2016. The June 2015 and June 2016 sampling events occurred during the dry-down phase of the annual hydrograph, and the August 2015 sample event was conducted during baseflow. Water samples were collected every 50 m throughout the McRae Creek mainstem and each of two key tributaries in all 3 sampling events (Fig. 1). The mainstem of McRae Creek was sampled from its confluence with Lookout Creek upstream for 8.1 km with 158 sampling locations per sampling event. Due to a series of waterfalls that limited safe access, samples were not collected from a 250 m section of McRae Creek mainstem (between meters 4000 and 4300). We additionally sampled through each of the two main tributaries on either side of the valley draining to the mainstem (Fig. 1). In McRae Creek Tributary-West (MCTW) we collected samples along 2.8 km of stream (57 sampling locations), and in McRae Creek Tributary-East (MCTE) we collected samples along 0.5 km of stream (11 sampling locations) during each collection period (Fig. 1). We also collected samples along 0.3 km of a tributary to MCTW (7 sampling locations per sampling event) extending from the confluence with MCTW upstream to the HJ Andrews W6 weir. The whole of the McRae Creek catchment is 1551 ha. MCTW is the largest sub-catchment and has an area of 258 ha, and MCTE has a catchment area of 120 ha (Fig. 1). Throughout the sampling area in McRae Creek mainstem, in MCTW, and in the tributary to MCTW, streams remained connected with surface flow. The lower section of MCTE also had connected surface waters, however the upper ~100 m of the survey reach in this tributary had some disconnected pools. At each sampling location, three replicate 30 ml water samples were collected from the thalweg. Each sample was filtered on site (Whatmann GF/F) and immediately stored on ice. Samples were frozen within 6 h for later analysis. All samples were run at the Oregon State University Institute for Water and Watersheds

Collaboratory on a Dionex ICS-1500 Ion Chromatograph for NO_3^- , PO_4^{3-} , and Cl^- . Chloride data are only available for August 2015 and June 2016. Nitrate and PO_4^{3-} are available for all 3 dates.

Data analysis

Our analyses assess spatial patterns in stream nutrient concentrations during each of the three sampling events and evaluate how differences in summer discharge affect the spatial variability of nutrient concentrations. We first explored longitudinal patterns in NO_3^- -N, PO_4^{3-} -P and Cl^- along stream distance in the mainstem and in each of the two tributaries over all three time periods (using average concentrations from the three replicates at each location). We then evaluated overall patterns in the molar NO_3^- -N: PO_4^{3-} -P ratio through the McRae Creek mainstem during each time period. This ratio analysis excludes NH_4^+ -N, which is an additional inorganic N source, however previous data from this system found low contribution of NH_4^+ to DIN in McRae Creek (Supplement 1). While this not a complete analysis of inorganic N:P ratios, the NO_3^- -N: PO_4^{3-} -P ratio here provides a broad picture of how dominant sources of inorganic N and P shift together along the mainstem stream. We also evaluated the spatial relationships of Cl^- , and of NO_3^- -N: Cl^- and PO_4^{3-} -P: Cl^- . Chloride is atmospherically-derived and is a conservative tracer which is not affected by biological processes or water-rock interaction. Concentrations of Cl^- vary as a function of differing evapotranspiration, and therefore can be used to identify hydrologic processes such as the storage, transport, and mixing of water masses.

To assess overall effects of flow conditions on nutrient concentration along larger river segments, we separated the network into three sections: (1) the mainstem of McRae Creek (from meter 0 at its confluence with Lookout Creek upstream to meter 8050); (2) MCTW, which encompassed MCTW upstream 2850 m to the gauging weir on H.J. Andrews Watershed 8 and an additional small (~300 m) section of a headwater tributary entering this stream and draining Watershed 6; and (3) MCTE, which included the 500 m second-order section of this stream. For each stream segment, we evaluated the mean, median, range, upper quartile, lower quartile, and coefficient of variation of both NO_3^- -N and PO_4^{3-} -P during each sample period and Cl^- during the August 2015

and June 2016 sampling events. To evaluate our hypothesis that the influence of both variability in local inputs and variability in local uptake would be enhanced in the net surface water nutrient concentrations during low flow conditions, we conducted an ANOVA comparing mean concentrations of each solute across the three survey periods. We also evaluated median concentration and the upper 90% and lower 10% of concentrations along each section during each sampling period.

To assess our hypothesis that stream nutrient concentrations would be more spatially variable at the network scale during extreme drought conditions, we conducted semi-variogram analyses following methods in McGuire et al. (2014) and Dent and Grimm (1999) for $\text{NO}_3\text{-N}$, $\text{PO}_4\text{-P}$, and Cl^- for the entire 11.5 km stream network during each sampling event. Semi-variogram analysis provides an aggregate measure of how variability scales with distance between sampling points (i.e. spatial autocorrelation). We used the R package SSN (VerHoef et al. 2014) with a lag interval of 4000 m [$\sim 1/2$ of the maximum distance between points (Journel and Huijbregts 1978) divided into 60 bins and a minimum of 20 pairs of sample points to estimate the semi-variance at each lag interval. Following Dent and Grimm (1999), we fitted a spherical model to the data and calculated the nugget (apparent y-intercept), sill, range, and initial slope of each semi-variogram to which a spherical model could be fit. The nugget represents sampling error or spatial variability that occurs at a spatial scale that is smaller than the sampling frame, (i.e., distance between sampling locations; 50 m in the current study) (Dent and Grimm 1999). The sill is the asymptote of the semi-variance, indicating that there is no longer spatial dependence in the data (in contrast to a continuous increase in semi-variance that occurs when values become increasingly divergent at increasing spatial scales) (Dent and Grimm 1999). In cases where a sill develops, the lag distance at which the asymptote occurs is the range and represents the distance at which there is no longer spatial autocorrelation for the metric of interest. Dent and Grimm (1999) considered this distance of spatial autocorrelation to be a measure of patch size in a stream, indicating a region that is different from its surroundings. The slope of the relationship between lag distance and semi-variance up to the sill is the strength of the degree of spatial dependence over the range

distance. In cases where a spherical model could not be fit, a linear fit is used. In these cases, there is no sill or range, but an intercept and slope can be fit for a comparison between years. If there is greater local variation in the concentration of a solute at a given distance interval, this will manifest as a larger semi-variance at that lag distance.

We expected increasing semi-variance as lag distance increases, indicating that solute concentrations are more dissimilar as the separation between points increases. If there is an asymptotic relationship between lag distance and semi-variance, the point at which semi-variance no longer increases with greater lag distance (i.e., the range) indicates that points separated by greater lag distances are no longer spatially auto-correlated. With greater demand for N than P in the larger stream network and a higher degree of local variability due to patchy inputs and areas of greater biological demand (“hotspots” of N input or uptake), we expect higher semi-variance values for $\text{NO}_3\text{-N}$ relative to $\text{PO}_4\text{-P}$ at each spatial scale (lag distance). Considering the different sampling periods, we expected more local variation and patchiness at lower flows for $\text{NO}_3\text{-N}$, which would manifest as larger semi-variance for the same lag distance in August 2015 relative to the other two sampling periods. We also expected that more extreme drought conditions would enhance the patch-scale influence of local hotspots of uptake or input of nitrogen, which would manifest as a steeper increase in semi-variance as lag distances increase. Further, if extreme drought conditions lead to a stronger influence of local hotspots on solute concentrations in the larger system, then we would expect to see a longer range for those solutes in the August 2015 data relative to the June 2015 or June 2016 data. Conversely, if the effects of a hotspot become more localized with decreasing flows, we would expect to see shorter ranges in August 2015 relative to June 2015 or June 2016.

Results

Hydrologic conditions

During our first sampling event in last week of June 2015, mean flow in the larger Lookout Creek basin into which McRae Creek drains was 400 L s^{-1} , which was 31% of the mean flow for that week based on

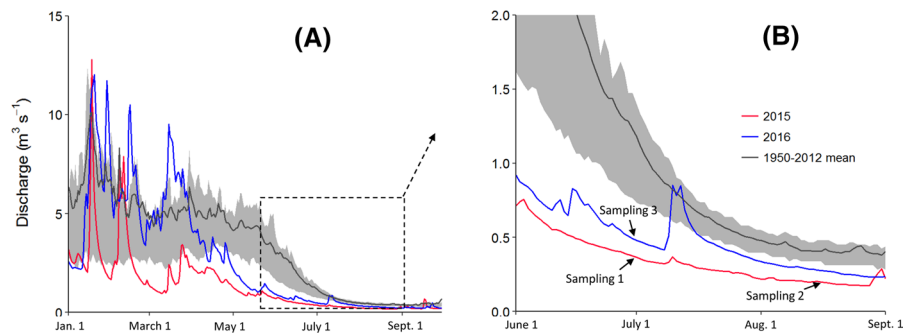


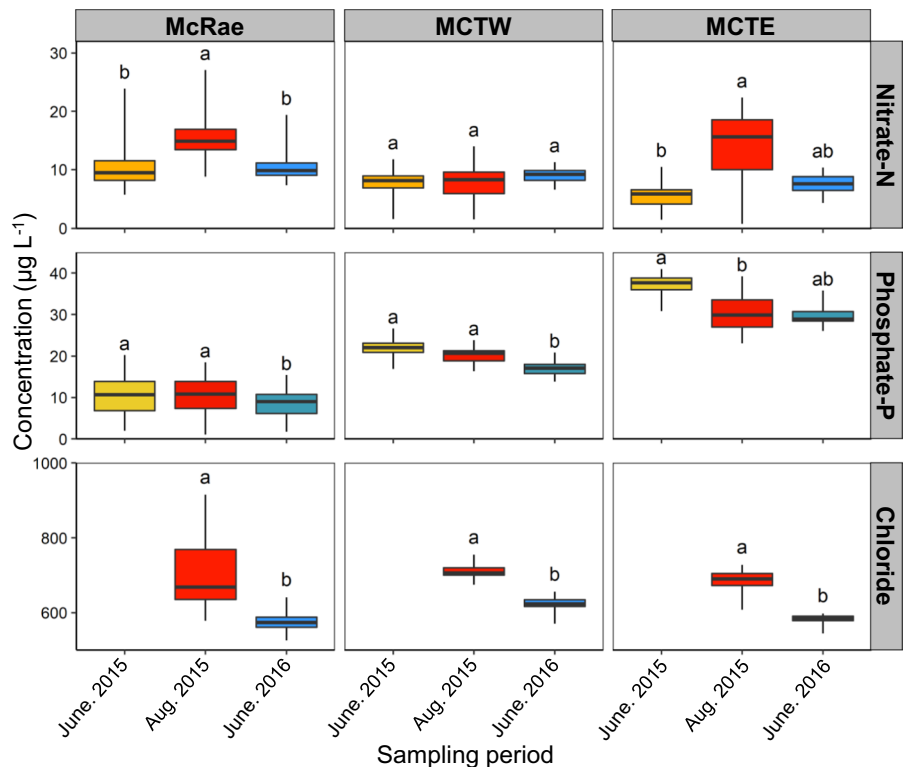
Fig. 2 Discharge at the Lookout Creek gauging station in the HJ Andrews Experimental Forest for 2015 (red), 2016 (blue) and the historic average from 1950 to 2012 (dark grey). The shaded area represents the central quartiles of the long-term

averages. Panel **A** includes the full calendar year. The dotted box in panel **A** encompassing just the June 1 to September 1 time period is expanded in Panel **B**. (Color figure online)

discharge records from 1950–2012 (Fig. 2). This was the 2nd lowest flow on record for this week of the year. During our second sampling period in the third week of August 2015, mean flow in the mainstem of Lookout Creek was 192 L s^{-1} , which was 48% of the mean discharge for this week over the 70-year record and the fifth-lowest discharge on record for this week of the year (Fig. 2). During our third sampling period

in the last week of June 2016, stream discharge at the Lookout Creek mainstem gauge was 545 L s^{-1} . This was greater than either of the 2015 sampling weeks (26% higher than late June 2015 and 65% higher than August 2015), however flows during this week were still 42% of the mean flow at this gauge in the last week in June, and the fourth lowest mean flow for the last week in June over the 70-year record.

Fig. 3 Boxplots of nitrate-N (upper panels), phosphate-P (middle panels), and chloride (lower panels) concentrations during the three sampling periods in McRae Creek mainstem, and tributaries MCTW, and MCTE. Plot whiskers indicate 10th and 90th percentiles. Letters indicate significance groupings from Tukeys HSD



Longitudinal patterns in solute concentrations and stoichiometric ratios

The mean concentration of NO_3^- -N was greatest during August 2015 in the McRae Creek mainstem and in MCTE stream segments (Fig. 3, Supplement 2). In the MCTW tributary, mean and median NO_3^- -N concentrations were similar across all three sampling events (Fig. 3; Supplement 2). At a finer scale, segments of the stream network exhibited different NO_3^- -N temporal patterns across the three sampling periods (Fig. 4). For example, some sections exhibited the lowest NO_3^- -N concentrations during the peak of the drought (i.e., McRae m 4300–5300, and MCTW m 1300–2000), whereas other sections had the highest NO_3^- -N concentrations during the peak drought (e.g., McRae m 2000–4300 and 6200–7500; MCTW m 2300–2500; MCTE m 0–300). The range of NO_3^- -N was largest in all three streams sections (mainstem McRae Creek and both tributaries) during August 2015. In all three network sections, variance in NO_3^- -N concentrations was lowest during the June 2016 sampling event when flows were highest (Fig. 3; Supplement 2).

One site in the upper section of the McRae Creek mainstem (at ~meter 8000) had substantially higher NO_3^- -N concentrations in August 2015 than any

other location (Fig. 4). This high concentration value was not apparent in any of the other surveys at this site, but all three replicate samples collected from this location at this time were similar in value, suggesting that this was an accurate measurement of a localized area of high N input that was only evident during the extreme low flow conditions. When this extreme outlier at meter 8000 is excluded, the range of concentrations between the highest and lowest value was similar during June and August of 2015. This outlier was removed from the semi-variogram analysis as it substantially skewed the data in those analyses, and therefore impacted our ability to address broader patterns across the network.

In the mainstem of McRae Creek and MCTW, mean stream PO_4^{3-} -P concentrations were slightly lower during June 2016 (when flows were greater than in either of the two 2015 sampling periods) (Fig. 3; Supplement 2). In MCTE, PO_4^{3-} -P concentrations were higher in June 2016, and largely comparable in August 2015 and June 2016. Along the mainstem, there was a clear longitudinal trend of increasing PO_4^{3-} -P concentrations moving downstream across all three sampling events (Fig. 5). The lowest P concentrations corresponded with the upper section of the McRae Creek mainstem with the highest inorganic N concentrations. Chloride concentrations were

Fig. 4 Spatial pattern of NO_3^- -N in June 2015, August 2015, and June 2016, throughout the mainstem, McRae Creek (A) and its two major tributaries, MCTW (B) and MCTE (C). The x-axis values represent A distance from confluence between McRae Creek and Lookout Creek, B distance from the confluence between MCTW and McRae Creek mainstem, and C distance from the confluence between MCTE and McRae Creek mainstem. Error bars are \pm one standard error from the three replicate samples collected at each location

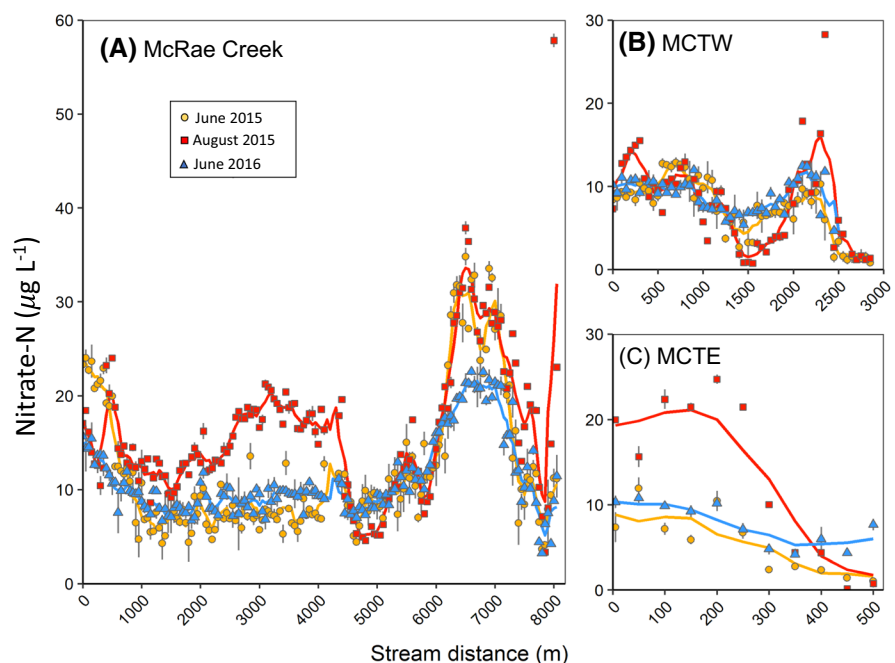


Fig. 5 Spatial pattern of $\text{PO}_4^{-3}\text{-P}$ in June 2015, August 2015, and June 2016, throughout the mainstem, McRae Creek (A) and its two major tributaries, MCTW (B) and MCTE (C). The x-axis values represent A distance from confluence between McRae Creek and Lookout Creek, B distance from the confluence between MCTW and McRae Creek mainstem, and C distance from the confluence between MCTE and McRae Creek mainstem. Error bars are \pm one standard error from the three replicate samples collected at each location

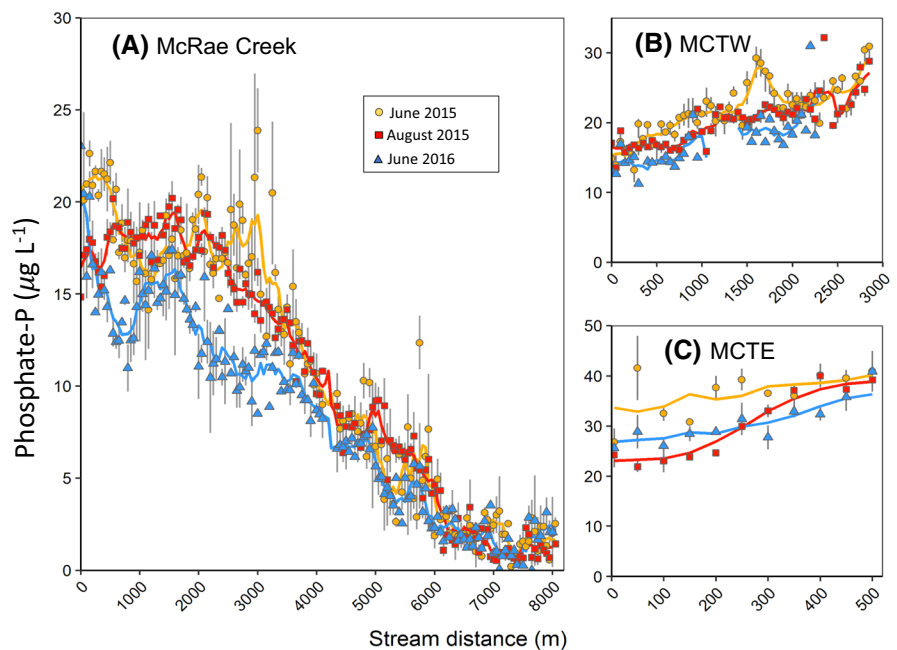
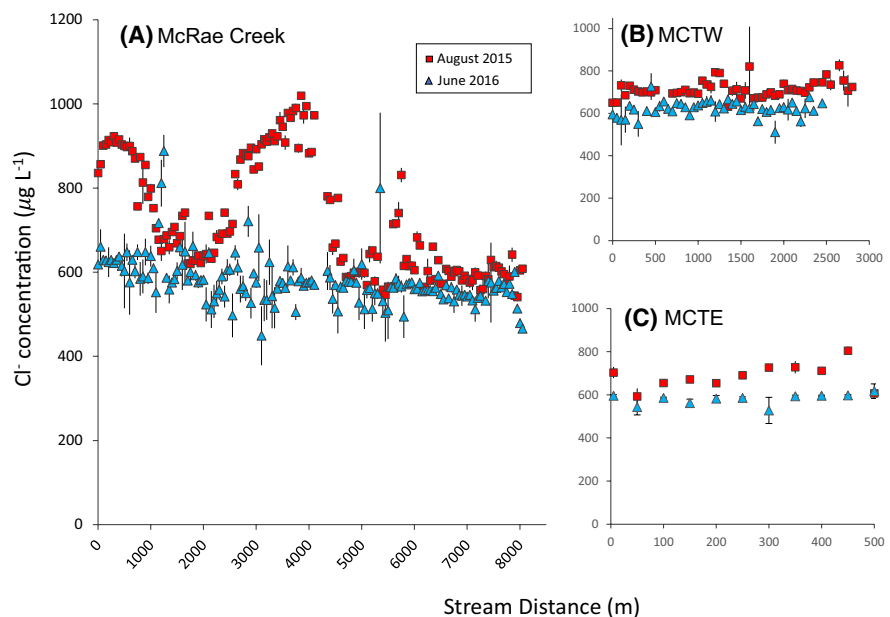


Fig. 6 Spatial pattern of chloride (Cl^-) in August 2015, and June 2016, throughout the mainstem, McRae Creek (A) and its two major tributaries, MCTW (B) and MCTE (C). The x-axis values represent A distance from confluence between McRae Creek and Lookout Creek, B distance from the confluence between MCTW and McRae Creek mainstem, and C distance from the confluence between MCTE and McRae Creek mainstem. Error bars are \pm one standard error from the three replicate samples collected at each location



greater during August 2015 than in June 2016 in all three stream sections (Fig. 3, Supplement 2). The Cl^- concentrations were particularly elevated in three areas of the mainstem ($\sim 0\text{--}1000$ m; $\sim 2800\text{--}4500$ m; and $\sim 5600\text{--}5900$ m) during the lowest drought flow in August 2015 relative to higher flows in June 2016 (Fig. 6; Supplement 3). In the two tributaries, although concentrations of Cl^- were higher during

August 2015, overall longitudinal patterns did not change.

The ratios of $\text{NO}_3^- \text{-N} : \text{PO}_4^{-3}\text{-P}$ were much higher in the upper part of the network, generally above 6000 m (Fig. 7). In an upper 2000 m section of McRae Creek mainstem (from ~ 6000 m to ~ 8000 m), the molar $\text{NO}_3^- \text{-N} : \text{PO}_4^{-3}\text{-P}$ ratios reached peaks of 55–67, which far exceeded in the rest of the stream

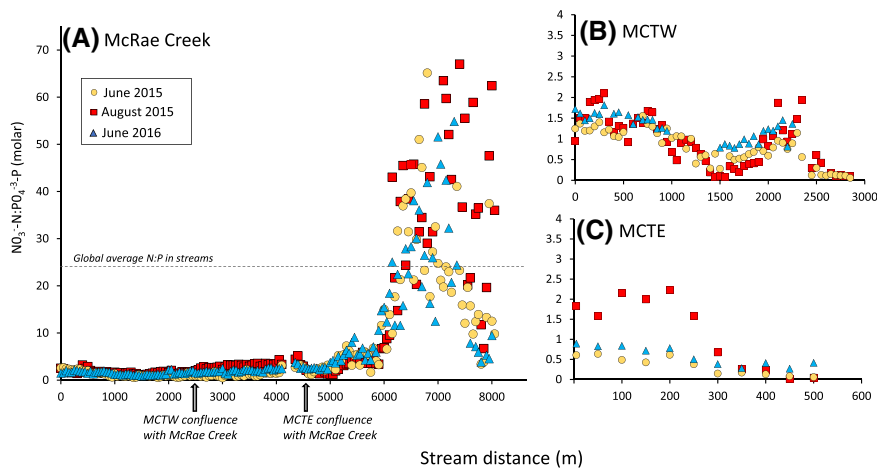


Fig. 7 Spatial pattern of the molar NO_3^- -N: PO_4^{3-} -P ratio in June 2015, August 2015, and June 2016, throughout the mainstem, McRae Creek (A) and its two major tributaries, MCTW (B) and MCTE (C). The ratio of 24:1 shown here is the global average N:P ratio in streams from Maranger et al. (2018). The

x-axis values represent A distance from confluence between McRae Creek and Lookout Creek, B distance from the confluence between MCTW and McRae Creek mainstem, and C distance from the confluence between MCTE and McRae Creek mainstem

network where ratios ranged from roughly 0.5 to 3.5. The pattern of elevated NO_3^- -N: PO_4^{3-} -P ratios in the upper section of McRae Creek was consistent across all three sampling events, but there were differences in the magnitude of the ratio and in the spatial extent of stream over which the NO_3^- -N: PO_4^{3-} -P ratios were elevated. The increase in NO_3^- -N: PO_4^{3-} -P ratios was largest during extreme low flow in August 2015. During this sampling period, NO_3^- -N: PO_4^{3-} -P ratios were dramatically elevated along the upper 2 km of McRae Creek (Fig. 6). This contrasts with both June 2015 and June 2016 sampling when a shorter section of the stream had elevated NO_3^- -N: PO_4^{3-} -P ratios (Fig. 7). The ratio of NO_3^- -N: Cl^- along McRae Creek mainstem was more variable in August 2015 than in June 2016 and as with the raw NO_3^- -N concentration data, there was a substantial increase in the upper 2000 m of McRae Creek mainstem (Supplement 4). The ratio of PO_4^{3-} -P: Cl^- was generally consistent with the overall trends in PO_4^{3-} -P concentration with general increases downstream on the mainstem of McRae Creek (Supplement 4).

Semi-variogram analysis

For NO_3^- -N, spherical models were a strong fit to semi-variograms and sill and range values could be estimated (Fig. 8A). The semi-variance sill

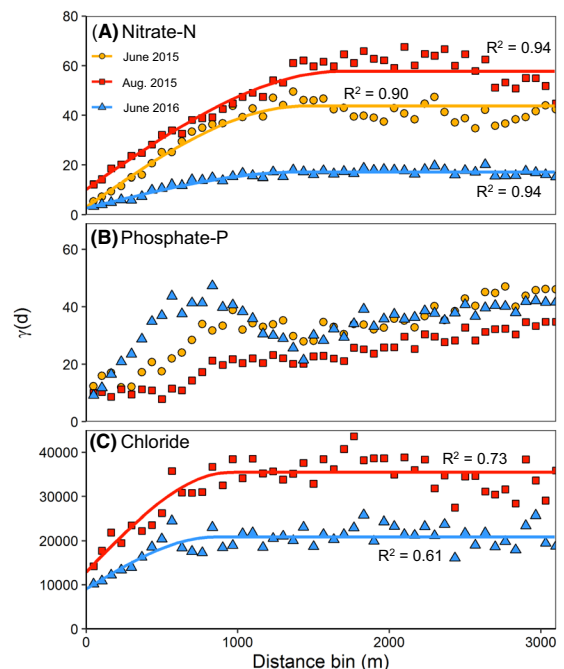


Fig. 8 Semi-variance of nitrate-N (A), phosphate-P (B), and chloride (C) through the McRae Creek network during moderate (June 2016) and severe (June and August 2015) drought conditions. Fitted lines are spherical models with the quality of the fit expresses as an r^2 value. The x-axis indicates lag distances between points for the semi-variance analysis

(asymptote) was greatest in August 2015, indicating that overall NO_3^- -N concentrations were more spatially variable during peak drought conditions (Supplement 3). The NO_3^- -N semi-variance lag distance (range) was approximately 1450 m in both June of 2015 and 2016 and up to approximately 1850 m in August 2015 (Supplement 3). These values indicate that spatial variability in NO_3^- -N concentrations along the stream sections increase up to distances between points of about ~1400 m in June of 2015 and 2016 and up to distances of ~1800 m apart in August 2015. Beyond these ranges, NO_3^- -N concentrations are spatially independent (i.e. concentrations at point x are not related to concentrations in the stream that are more than ~1400 or ~1800 m away—the range distance). Overall, these empirical semi-variograms indicate that during the drought local NO_3^- -N concentrations were more different from each other and were spatially autocorrelated for longer lag distances compared to periods of higher flows.

The PO_4 -P semi-variance patterns differed in multiple ways from NO_3^- -N (Fig. 8B). In contrast to NO_3^- -N, over distance intervals (range) up to 1500 m, we observed the greatest semi-variance of PO_4 -P during the period with highest flow (June 2016) and the least semi-variance in the period with the lowest flow (August 2015; Fig. 8B). The PO_4^{-3} -P semi-variograms did not reach an asymptote during any sampling period (indicating spatial dependence at all lag distances throughout the network). Consequently, these semi-variograms are best represented by a linear model, and spherical model parameters (e.g. range and sill) could not be obtained.

As with the NO_3^- -N, variation in the concentrations of Cl^- was greater across all spatial scales during August 2015 as compared to the higher flow conditions of June 2016 (Fig. 8C). The range was also larger in August 2015 (949 m) than in June 2016 (845 m), although the difference in range between the two time periods was much smaller for Cl^- than for NO_3^- -N (~100 m for Cl^- versus ~400 m for NO_3^- -N).

Discussion

Nutrient availability is an important control on primary production and heterotrophic respiration rates in aquatic ecosystems. In streams, a number of studies

have documented how nutrient concentrations can affect ecosystem processes (Bernhardt et al. 2018; Bernot et al. 2010; Rosemond et al. 2015, 2000), and conversely, how ecosystem processes can influence nutrient concentrations (Bernhardt et al. 2005; Hall and Tank 2003), which can affect nutrient availability patterns at larger spatial scales (Dong et al. 2017; Dupas et al. 2019; Tank et al. 2018). Therefore, understanding spatial and temporal patterns of stream nutrient availability throughout stream networks can inform our understanding of the spatial dynamics of stream ecosystem processes including primary production, respiration, and ultimately stream solute fluxes (Abbott et al. 2018; Hoellein et al. 2011; Raymond et al. 2013; Rosemond et al. 2015). In the McRae Creek semi-variogram analysis results indicated that watershed spatial variability of the most commonly limiting nutrient [nitrogen (N) as NO_3^- -N] increased during a severe summer drought. We attribute this increase in spatial heterogeneity to reduced surface water dilution and transport associated with decreasing streamflow, which in turn enhanced the relative influence of local input and retention processes on stream NO_3^- -N concentrations along the network.

The increased importance of localized areas of nutrient processing, as well as increased river network regulation of the key nutrient under lower flow conditions is most clearly illustrated in the NO_3^- -N concentration pattern with longitudinal stream distance in the McRae Creek mainstem (Fig. 4). During the very lowest flows in August 2015, the highest concentrations of NO_3^- -N occurred between meters 6500 and 7000, while some of the lowest concentrations are present just a few kilometers downstream between meters 4500 and 5000. This is consistent with earlier stream research documenting the role of stream ecosystem processes in affecting nutrient availability (e.g. Dent and Grimm 1999; Hall and Tank 2003; Bernhardt et al. 2005; Hoellein et al. 2011; Gomez-Gener et al. 2020). The pattern of higher highs and lower lows of NO_3^- -N concentrations was also evident in the McRae Creek tributary MCTW during the lowest flow conditions in August 2015. In MCTE, total NO_3^- -N concentrations were lower during the lowest flow conditions in August 2015, which we also attribute to increased importance of local processing during baseflow drought conditions.

This pattern of decreasing $\text{NO}_3\text{-N}$ is also apparent when stream $\text{NO}_3\text{-N}$ concentrations are normalized to Cl^- concentrations suggesting that net decline in concentration is not accounted for by simple dilution or evaporative processes alone. Chloride concentrations can be used to determine if multiple groundwater regimes exist, and if so, changing Cl^- concentrations can indicate shifts in the proportions of groundwater derived from those different regimes (Mengis et al. 1999). The lack of change in Cl^- concentrations in the upper portion of the network from m 7000–6000 on the mainstem of McRae Creek suggests that no major shifts occurred in the relative contributions of deep groundwater versus potential shallower flowpaths along this section of the upper mainstem (Fig. 6), despite a possible transition between bedrock units along this section (Bywater-Reyes et al. 2017). Similarly, $\text{NO}_3\text{-N}:\text{Cl}^-$ ratios can be used to tease apart dilution versus consumption or production processes (Altman and Parizek 1995; Devito et al. 2000). The decline in both $\text{NO}_3\text{-N}$ and in $\text{NO}_3\text{-N}:\text{Cl}^-$ ratios in the upper section implies either that water inputs have experienced greater denitrification with increasing downstream longitudinal distance, or that greater in-stream net $\text{NO}_3\text{-N}$ uptake occurs along this reach. While not conclusive, together these data suggest that these strong declines in net $\text{NO}_3\text{-N}$ concentrations were likely driven by $\text{NO}_3\text{-N}$ processing during the low flow conditions.

In contrast to the upper section of the McRae Creek mainstem, in the middle and lower section of this stream we saw significant variations in Cl^- concentrations, which suggests that differing groundwater inputs play a larger role in controlling spatial patterns of solutes in this section. The changing concentrations of nitrate in the lower section of McRae are tightly coupled with Cl whereas they are largely decoupled in the upper reach. This leads to a $\text{NO}_3\text{-N}:\text{Cl}^-$ ratio that increases in the upper reach, but is relatively constant in the lower section of the mainstem. These differences suggest that in some sections of the stream spatial variability of N during a drought is driven by changes in the proportion of different groundwater input sources whereas in other sections of the stream spatial variability is more likely to be driven by unique chemistry of groundwater inputs or in-stream processing.

The spatial patterns of $\text{PO}_4\text{-P}$ concentrations across the stream network were largely similar during

all three sampling periods indicating that overall patterns of $\text{PO}_4\text{-P}$ availability in this network were comparable during dry-down period and baseflow conditions of an extreme drought (Fig. 5). The dominant spatial pattern in $\text{PO}_4\text{-P}$ is of increasing concentration with downstream distance. This longitudinal pattern may be related to the transition between the two bedrock units, either relating to a difference in bedrock P chemistry or in hydrologic flowpaths and/or residence times. While spatial patterns were relatively consistent, there were still temporal differences in absolute $\text{PO}_4\text{-P}$ concentrations among the three low flow periods. Throughout most of the lower mainstem of McRae Creek (m 0–6000), mean concentrations of $\text{PO}_4^{3-}\text{-P}$ were generally comparable between June and August of 2015, but were lower in June 2016 when flows were highest. In the upper mainstem (m 6000–8500), concentrations were similar not only in both 2015 sampling events, but also in June 2016. When normalized to Cl^- , $\text{PO}_4^{3-}\text{-P}$ spatial patterns in the mainstem showed a similar pattern as the raw concentration data (Supplement 5). This contrasts the $\text{NO}_3\text{-N}$ data where differences in availability along the stream were diminished but still clearly present when normalized to Cl^- . We attribute this P behavior to the fact that in most of the network, except—for the section of the mainstem between 6000 and 8000 m— $\text{PO}_4\text{-P}$ does not appear to be a limiting nutrient.

In Pacific Northwest headwater stream ecosystems, N is the most common limiting nutrient (Aumen et al. 1983; Warren et al. 2017), and throughout the majority of the mainstem McRae Creek, MCTW and MCTE, the $\text{NO}_3\text{-N}:\text{PO}_4\text{-P}$ ratio is low (roughly ≤ 2) for all three sampling events. Limitation of N versus P in stream ecosystems cannot be reduced to just a simple ratio due to variations in nutrient requirements among various autotrophs within a community, and plasticity in nutrient acquisition and retention with changing nutrient availability (Maranger et al. 2018). However, stream nutrient enrichment experiments generally indicate that N limitation exists when N:P ratios are lower (closer to 1:1), and that P limitation exists when N:P ratios are higher (closer to 100:1) (Keck and Lepori 2012). Based on this understanding of the stream nutrient limitation context, most of the McRae network was likely N-limited during all three low-flow conditions, a result consistent with previous assessments of nutrient limitation using bioassays under adequate light conditions (Warren et al. 2017).

Although most of the stream network appeared to be N-limited, an approximately 1.5 km section of the upper mainstem of McRae Creek was potentially P-limited. In this stream section, the spatial and temporal patterns in the $\text{NO}_3\text{-N}:\text{PO}_4\text{-P}$ ratio changed substantially across the three flow conditions, and the area of potential P limitation increased substantially during extreme low flow conditions in August 2015 relative to the other sampling periods (Fig. 7). We suggest that this is due to more consistent input of inorganic N (either as NO_3^- or as NH_4^+ which is then nitrified) from deep groundwater flowpaths that are no longer (or to a lesser degree) diluted by surface waters and shallow flowpaths during baseflow of an extreme drought. This is consistent with lower degree of hydrologic connectivity to older ground water that resulted in shorter mean transit times for 2015 compared to 2016–2018 (Segura 2021). Because we do not have bioassay results from this upper section of the McRae Creek mainstem or NH_4^+ data that would allow us to determine the total concentration of inorganic N, we cannot definitively suggest a point at which this system shifts to P-limitation. However, a potential transition to P-limitation is likely in areas along this section of McRae Creek based on $\text{NO}_3\text{-N}:\text{PO}_4\text{-P}$ ratios that regularly exceed 30. Further, in this reach above meter 6000 along the mainstem of McRae Creek where nitrate concentrations were elevated, $\text{PO}_4\text{-P}$ concentrations were lower at a majority of sampling locations during the most extreme drought, which is consistent with the interpretation of potential P limitation.

The contrast between $\text{NO}_3\text{-N}$ and $\text{PO}_4\text{-P}$ behavior reflects the distinct sources and reactivity of each solute. Nitrate is an almost entirely biogenic solute and is actively biologically cycled in both soils and stream water. Phosphate is both geogenic (derived from rock weathering), biologically cycled in both soils and stream water, and susceptible to adsorption on stream sediments. A comparison of Cl^- , NO_3^- , and PO_4^{3-} between extreme drought conditions and more moderate low-flow conditions (August 2015 relative to June 2016, with $\sim 2.5\times$ differences in discharge) indicates that in addition to input processes from groundwater sources or in-stream nitrification becoming increasingly important in enhancing spatial variability of stream nutrient solutes (per Segura et al. 2019), for a limiting nutrient, the role of local

biological processes in driving patterns of spatial variability also increases and may exceed input effects in extreme low flows. For a non-limiting nutrient ($\text{PO}_4^{3-}\text{-P}$ in the majority of the network in this study), inputs seemed to dominate over in-stream processing. The finding that the more limiting nutrient exhibits greater spatial variability is consistent with Hoellein et al.'s (2011) work in the Bronx River in New York where P was more often limiting than N and $\text{PO}_4^{3-}\text{-P}$ also exhibited greater spatial variability.

The semi-variograms illustrate how nutrient concentrations in a given location relate to nutrient concentrations in a series of binned distances away from that point. Greater variability between nearby points yield greater semi-variance values, while cases in which concentrations at one point are more similar to those nearby (and at a series of distance intervals away) will yield lower semi-variance. The increase in semi-variance of $\text{NO}_3\text{-N}$ at all spatial scales during August 2015 baseflow, relative to the summer dry-down phase of a drought in June 2015 and June 2016 indicated greater spatial variability of this solute and was generally consistent with seasonal patterns observed in southwestern streams as flows declined through the summer (Fig. 8A) (Dent and Grimm 1999). While the pattern in semi-variance across a range of distance intervals was similar in June 2015 and August 2015, the magnitude of the semi-variance was lower in June of this year, suggesting that a similar process was occurring but had not fully developed early in the summer. The pattern held in June 2016 as well but was further diminished. This was somewhat surprising given that flows at this time were still well below average. In addition to greater semi-variance values for a given lag distance (distance interval between points), the distance over which stream nitrate concentrations were related to one another—the range—was also larger in August 2015, indicating that patterns in nutrient concentration of $\text{NO}_3\text{-N}$ manifested over a longer distance in the stream during baseflow of this extreme drought. Although the semi-variance analysis indicates strong response in the spatial characteristics of nutrient availability during an extreme drought, it does not address mechanism. Further work is needed across a wider range of flows and with more direct assessment of adjacent groundwater to add more context to these data in regard to discharge conditions and factors that may affect the spatial dynamics of a limiting nutrient. The relative lack

of pattern and increased homogeneity during extreme low flow in the semi-variance analysis of $\text{PO}_4^{-3}\text{-P}$ is consistent with our expectations for a nutrient that is broadly and more homogeneously sourced and largely not limiting (Fig. 8B). The clear establishment of a sill in the semi-variance of Cl^- suggests that during a drought localized areas of groundwater input become increasingly influential, but that this effect is lost at a scale of about 700 m (Fig. 8C). This result is consistent with a hydrologic analysis of the larger Lookout Creek stream system during the 2015 drought (Segura et al. 2019).

Our results are consistent with recent work from Sweden, which suggested that changes in flow during droughts can promote shifts in local biogeochemical processes that can impact the larger network (Gomez-Gener et al. 2020). And, beyond implications for ecological processing along a network, the observed increases in spatial heterogeneity of a key limiting nutrient (inorganic N) during a drought also has practical implications for data collection efforts that are intended to characterize stream spatial dynamics. In regard to the status of a limiting nutrient, results suggest that the spatial scope of inference from a single sampling location reflects longer stream sections during high flows and shorter sections during low-flows. Characterizing the spatial patterns of a nutrient in a given stream therefore requires fewer samples during high flows than during low-flows. This pattern toward homogenization of stream nutrients as flow increases is similar to those seen for stream temperature where low flows create greater spatial variability as the relative importance of groundwater dominated tributaries and groundwater input areas along the stream increase (Segura et al. 2019; Steel et al. 2019). However, in addition to input-driven differences, nutrient uptake is also important and sampling background nutrient concentrations during moderate or high flows—at high or low resolution—will likely miss key areas of both in-stream nutrient input or retention. In addition to changes in the spatial scope of inference around a single point, differences in spatial autocorrelation between sampling points at different flows may influence sampling efforts when using spatial interpolation tools such as spatial stream network (SSN) models (Isaak et al. 2014). The number of sampling locations required to achieve a given degree of accuracy will be denser during low-flows compared to higher flows as fine-scale heterogeneity may be missed more easily.

At low stream discharge, or over longer time periods when spatial dynamics are often more stable (Abbott et al. 2018; Dupas et al. 2019) areas of high input and high retention that were not apparent during higher flows can be clearly identified.

The observations in this study can be placed in the context of the River Network Saturation concept, which invokes hydrologic changes as a key driver that alters the balance between nutrient supply and demand (uptake by physical, chemical, or biological processes) (Wollheim et al. 2018). In this framework, nutrient supply is expected to exceed demand in headwater streams during high flows, and alignment between supply and demand is expected to increase as flows decline. The concept has been evaluated across flows that encompass standard baseflow and flood events (Bernal et al. 2019), as well as in the context of community succession in recovery from high flow events (Dent and Grimm 1999; Wollheim et al. 2018). However, there is limited data available to directly assess the influence of drought conditions on the spatial patterns of nutrients in stream networks. At the network scale, our $\text{NO}_3^- \text{-N}$ data support the hypothesis that nutrient supply and demand are well-connected during the drought. However, at smaller spatial scales, our data suggests that supply and demand for $\text{NO}_3^- \text{-N}$ actually became increasingly decoupled during the drought as local processes of input and loss become disproportionately important. Even though our system remained connected by surface flow during the drought, the dominance of local processes led to increasing spatial variability of $\text{NO}_3^- \text{-N}$ with some patches having higher demand relative to supply and others having higher supply relative to demand. For $\text{PO}_4^{-3}\text{-P}$, supply effects appeared to dominate over in-stream processing effects across all flows resulting in low spatial heterogeneity, but the demand for P was much lower in our study system than demand for N.

Conclusions

Drought is projected to be an increasingly frequent and severe disturbance in the Pacific Northwest of North America and indeed around the world in the coming decades. In stream ecosystems, determining how declining flows affect the spatial heterogeneity of stream nutrient concentrations has important implications for understanding how droughts will

affect spatial and temporal processes influenced by stream nutrient availability such as carbon processing, primary production, and nutrient export. Within the McRae Creek stream network in the Oregon Cascade Mountains, flow-mediated effects of the drought on spatial dynamics were more pronounced for the limiting nutrient (NO_3^-) compared to the non-limiting nutrient (PO_4^{3-}). The differences in the responses of N and P in our system also led to shifts in the potential amount and degree of N-limitation (and potentially P-limitation) with network position. While the system was predominantly N-limited, a hotspot of N input created a localized section where P-limitation likely occurred during low flows. Our study demonstrates that low-flow drought conditions that are expected to become increasingly common under future climate regimes can alter the spatial dynamics of stream nutrients. Under these conditions, not only is there a shift in local availability of a limiting nutrient, but the differential response of nutrients alters stream stoichiometry along a network.

Acknowledgements We thank Brian VerWey, Graham Takacs, Gavin Jones, and Lauren Still for their contributions to sample collection throughout the McRae Creek stream network. We thank Kathy Motter and the Oregon State University Collaboratory for technical support and access to facilities where water sample analyses were conducted. K. MacNeill and two anonymous reviewers provided helpful feedback on an earlier draft of this manuscript. We thank Lina DiGregorio, Mark Schulze and the HJ Andrews LTER for logistical support throughout the project.

Author contributions All authors contributed to the study conception and design. Material preparation and data collection were performed by EH, MK, and DW. Data analysis was performed by MK, JP-R, and CS. The first draft of the manuscript was written by DW and all authors commented extensively and materially on multiple subsequent drafts. All authors read and approved the final manuscript.

Funding This research was supported by National Science Foundation (NSF) grant DEB 1547628 and by an NSF Graduate Research Fellowship award. Facilities and funding for student technicians were provided by the HJ Andrews Experimental Forest and Long-Term Ecological Research (LTER) program, administered cooperatively by the USDA Forest Service Pacific Northwest Research Station, Oregon State University, and the Willamette National Forest and which is supported by the National Science Foundation under the LTER Grant Nos. LTER8 DEB-2025755 (2020–2026) and LTER7 DEB-1440409 (2012–2020).

Data availability The core dataset for this study is available through the HJ Andrews Experimental Forest website (<https://andrewsforest.oregonstate.edu/data>).

Declarations

Conflict of interest None of the authors have any competing interests related to this research.

References

- Abbott BW, Gruau G, Zarnetske JP, Moatar F, Barbe L, Thomas Z, Fovet O, Kolbe T, Gu S, Pierson-Wickmann AC, Davy P, Pinay G (2018) Unexpected spatial stability of water chemistry in headwater stream networks. *Ecol Lett* 21(2):296–308. <https://doi.org/10.1111/ele.12897>
- Altman SJ, Parizek RR (1995) Dilution of nonpoint-source nitrate in groundwater. *J Environ Qual* 24(4):707–718. <https://doi.org/10.2134/jeq1995.00472425002400040023x>
- Aumen NG, Bottomley PJ, Ward GM, Gregory SV (1983) Microbial decomposition of wood in streams—distribution of microflora and factors affecting [C-14]lignocellulose mineralization. *Appl Environ Microb* 46(6):1409–1416. <https://doi.org/10.1128/Aem.46.6.1409-1416.1983>
- Bernal S, Lupon A, Ribot M, Sabater F, Marti E (2015) Riparian and in-stream controls on nutrient concentrations and fluxes in a headwater forested stream. *Biogeochemistry* 12(6):1941–1954. <https://doi.org/10.5194/Bg-12-1941-2015>
- Bernal S, Lupon A, Wollheim WM, Sabater F, Poblador S, Marti E (2019) Supply, demand, and in-stream retention of dissolved organic carbon and nitrate during storms in Mediterranean forested headwater streams. *Front Env Sci-Switz* 7:ARTN 60. <https://doi.org/10.3389/fenvs.2019.00060>
- Bernhardt ES, Likens GE, Hall RO, Buso DC, Fisher SG, Burton TM, Meyer JL, McDowell MH, Mayer MS, Bowden WB, Findlay SEG, Macneale KH, Stelzer R, Lowe WH (2005) Can't see the forest for the stream?—In-stream processing and terrestrial nitrogen exports. *Bioscience* 55(3):219–230
- Bernhardt ES, Heffernan JB, Grimm NB, Stanley EH, Harvey JW, Arroita M, Appling AP, Cohen MJ, McDowell WH, Hall RO, Read JS, Roberts BJ, Stets EG, Yaculic CB (2018) The metabolic regimes of flowing waters. *Limnol Oceanogr* 63:S99–S118. <https://doi.org/10.1002/lno.10726>
- Bernot MJ, Sobota DJ, Hall RO, Mulholland PJ, Dodds WK, Webster JR, Tank JL, Ashkenas LR, Cooper LW, Dahm CN, Gregory SV, Grimm NB, Hamilton SK, Johnson SL, McDowell WH, Meyer JL, Peterson B, Poole GC, Vallett HM, Arango C, Beaulieu JJ, Burgin AJ, Crenshaw C, Helton AM, Johnson L, Merriam J, Niederlehner BR, O'Brien JM, Potter JD, Sheibley RW, Thomas SM, Wilson K (2010) Inter-regional comparison of land-use effects on stream metabolism. *Freshw Biol* 55(9):1874–1890. <https://doi.org/10.1111/j.1365-2427.2010.02422.x>

- Bywater-Reyes S, Segura C, Bladon KD (2017) Geology and geomorphology controls suspended sediment yield and modulate increases following timber harvest in temperate headwater streams. *J Hydrol* 548:754–769
- Cairns MA, Lajtha K (2005) Effects of succession on nitrogen export in the west-central Cascades. *Oregon Ecosyst* 8(5):583–601. <https://doi.org/10.1007/s10021-003-0165-5>
- Capps KA, Booth MT, Collins SM, Davison MA, Moslemi JM, El-Sabaawi RW, Simonis JL, Flecker AS (2011) Nutrient diffusing substrata: a field comparison of commonly used methods to assess nutrient limitation. *J N Am Benthol Soc* 30(2):522–532. <https://doi.org/10.1899/10-146.1>
- Compton JE, Church MR, Larned ST, Hogsett WE (2003) Nitrogen export from forested watersheds in the Oregon Coast Range: the role of N-2-fixing red alder. *Ecosystems* 6(8):773–785. <https://doi.org/10.1007/s10021-002-0207-4>
- Davis CA, Ward AS, Burgin AJ, Loecke TD, Riveros-Iregui DA, Schnoebelen DJ, Just CL, Thomas SA, Weber LJ, St Clair MA (2014) Antecedent moisture controls on stream nitrate flux in an agricultural watershed. *J Environ Qual* 43(4):1494–1503. <https://doi.org/10.2134/jeq2013.11.0438>
- Dent CL, Grimm NB (1999) Spatial heterogeneity of stream water nutrient concentrations over successional time. *Ecology* 80(7):2283–2298
- Devito KJ, Fitzgerald D, Hill AR, Aravena R (2000) Nitrate dynamics in relation to lithology and hydrologic flow path in a river riparian zone. *J Environ Qual* 29(4):1075–1084. <https://doi.org/10.2134/jeq2000.00472425002900040007x>
- Dong XL, Ruhi A, Grimm NB (2017) Evidence for self-organization in determining spatial patterns of stream nutrients, despite primacy of the geomorphic template. *Proc Natl Acad Sci USA* 114(24):E4744–E4752. <https://doi.org/10.1073/pnas.1617571114>
- Dupas R, Minaudo C, Abbott BW (2019) Stability of spatial patterns in water chemistry across temperate ecoregions. *Environ Res Lett* 14(7):ARTN 074015. <https://doi.org/10.1088/1748-9326/ab24f4>
- Gomez-Gener L, Lupon A, Laudon H, Sponseller RA (2020) Drought alters the biogeochemistry of boreal stream networks. *Nat Commun* 11(1):1795
- Hall RO, Tank JL (2003) Ecosystem metabolism controls nitrogen uptake in streams in Grand Teton National Park, Wyoming. *Limnol Oceanogr* 48(3):1120–1128. <https://doi.org/10.4319/lo.2003.48.3.1120>
- Hill WR, Knight AW (1988) Nutrient and light limitation of algae in 2 Northern California streams. *J Phycol* 24(2):125–132
- Hoellein TJ, Arango CP, Zak Y (2011) Spatial variability in nutrient concentration and biofilm nutrient limitation in an urban watershed. *Biogeochemistry* 106(2):265–280. <https://doi.org/10.1007/s10533-011-9631-x>
- Hur J, Schlautman MA, Karanfil T, Smink J, Song H, Klaine SJ, Hayes JC (2007) Influence of drought and municipal sewage effluents on the baseflow water chemistry of an upper Piedmont river. *Environ Monit Assess* 132(1–3):171–187. <https://doi.org/10.1007/S10661-006-9513-1>
- IPCC (2021) Climate Change 2021: the physical science basis. In: Masson-Delmotte V, Zhai P, Pirani A, Connors SL, Péan C, Berger S, Caud N, Chen Y, Goldfarb L, Gomis MI, Huang M, Leitzell K, Lonnoy E, Matthews JBR, Maycock TK, Waterfield T, Yelekçi O, Yu R, Zhou B (eds) Contribution of working group I to the Sixth Assessment Report of the Intergovernmental Panel on Climate Change. Cambridge University Press, Cambridge
- Isaak DJ, Peterson EE, Hoef JMV, Wenger SJ, Falke JA, Torgersen CE, Sowder C, Steel EA, Fortin MJ, Jordan CE, Ruesch AS, Som N, Monestiez P (2014) Applications of spatial statistical network models to stream data. *Wires Water* 1(3):277–294. <https://doi.org/10.1002/wat2.1023>
- Journel AG, Huijbregts CJ (1978) Mining geostatistics. The Blackburn Press, New York
- Kane ES, Betts EF, Burgin AJ, Clilverd HM, Crenshaw CL, Fellman JB, Myers-Smith IH, O'Donnell JA, Sobota DJ, Van Verseveldt WJ, Jones JB (2008) Precipitation control over inorganic nitrogen import-export budgets across watersheds: a synthesis of long-term ecological research. *Ecology* 89(2):105–117. <https://doi.org/10.1002/Eco.10>
- Kaylor MJ, Warren DR (2017) Linking riparian shade and the legacies of forest management to fish and vertebrate biomass in forested streams. *Ecosphere* 8(6):e01845
- Kaylor MJ, Warren DR, Kiffney PM (2017) Long-term effects of riparian forest harvest on light in Pacific Northwest (USA) streams. *Freshw Sci* 36(1):1–13. <https://doi.org/10.1086/690624>
- Keck F, Lepori F (2012) Can we predict nutrient limitation in streams and rivers? *Freshw Biol* 57(7):1410–1421
- Leibowitz SG, Comeleo RL, Wigington PJ, Weaver CP, Morefield PE, Sproles EA, Ebersole JL (2014) Hydrologic landscape classification evaluates streamflow vulnerability to climate change in Oregon, USA. *Hydrol Earth Syst Sci* 18(9):3367–3392. <https://doi.org/10.5194/Hess-18-3367-2014>
- Likens GE, Buso DC (2006) Variation in streamwater chemistry throughout the Hubbard Brook Valley. *Biogeochemistry* 78(1):1–30
- Maranger R, Jones SE, Cotner JB (2018) Stoichiometry of carbon, nitrogen, and phosphorus through the freshwater pipe. *Limnol Oceanogr Lett* 3(3):89–101. <https://doi.org/10.1002/lo2.10080>
- Mast MA, Clow DW, Baron JS, Wetherbee GA (2014) Links between N deposition and nitrate export from a high-elevation watershed in the Colorado front range. *Environ Sci Technol* 48(24):14258–14265. <https://doi.org/10.1021/Es502461k>
- McGuire KJ, Torgersen CE, Likens GE, Buso DC, Lowe WH, Bailey SW (2014) Network analysis reveals multiscale controls on streamwater chemistry. *Proc Natl Acad Sci USA* 111(19):7030–7035. <https://doi.org/10.1073/Pnas.1404820111>
- Mengis M, Schiff SL, Harris M, English MC, Aravena R, Elgood RJ, MacLean A (1999) Multiple geochemical and isotopic approaches for assessing ground water NO₃⁻ elimination in a riparian zone. *Ground Water* 37(3):448–457. <https://doi.org/10.1111/j.1745-6584.1999.tb01124.x>
- Mote PW, Rupp DE, Li SH, Sharp DJ, Otto F, Uhe PF, Xiao M, Lettenmaier DP, Cullen H, Allen MR (2016) Perspectives on the causes of exceptionally low 2015 snowpack in the

- western United States. *Geophys Res Lett* 43(20):10980–10988. <https://doi.org/10.1002/2016gl069965>
- Peterson BJ, Wollheim WM, Mulholland PJ, Webster JR, Meyer JL, Tank JL, Marti E, Bowden WB, Valett HM, Hershey AE, McDowell WH, Dodds WK, Hamilton SK, Gregory S, Morrall DD (2001) Control of nitrogen export from watersheds by headwater streams. *Science* 292(5514):86–90
- Raymond PA, Hartmann J, Lauerwald R, Sobek S, McDonald C, Hoover M, Butman D, Striegl R, Mayorga E, Humborg C, Kortelainen P, Durr H, Meybeck M, Ciais P, Guth P (2013) Global carbon dioxide emissions from inland waters. *Nature* 503(7476):355–359. <https://doi.org/10.1038/Nature12760>
- Rosemond AD, Mulholland PJ, Brawley SH (2000) Seasonally shifting limitation of stream periphyton: response of algal populations and assemblage biomass and productivity to variation in light, nutrients, and herbivores. *Can J Fish Aquat Sci* 57(1):66–75. <https://doi.org/10.1139/Cjfas-57-1-66>
- Rosemond AD, Benstead JP, Bumpers PM, Gulis V, Komonoski JS, Manning DWP, Suberkropp K, Wallace JB (2015) Experimental nutrient additions accelerate terrestrial carbon loss from stream ecosystems. *Science* 347(6226):1142–1145. <https://doi.org/10.1126/Science.Aaa1958>
- Segura C (2021) Snow drought reduces water transit times in headwater streams. *Hydrol Processes* 35(12):ARTN e14437. <https://doi.org/10.1002/hyp.14437>
- Segura C, Noone D, Warren D, Jones JA, Tenny J, Ganio LM (2019) Climate, landforms, and geology affect baseflow sources in a mountain catchment. *Water Resour Res* 55(7):5238–5254. <https://doi.org/10.1029/2018wr023551>
- Sheffield J, Wood EF (2008) Global trends and variability in soil moisture and drought characteristics, 1950–2000, from observation-driven simulations of the terrestrial hydrologic cycle. *J Clim* 21(3):432–458
- Sproles EA, Nolin AW, Rittger K, Painter TH (2013) Climate change impacts on maritime mountain snowpack in the Oregon Cascades. *Hydrol Earth Syst Sci* 17(7):2581–2597. <https://doi.org/10.5194/Hess-17-2581-2013>
- Steel EA, Marsha A, Fullerton AH, Olden JD, Larkin NK, Lee SY, Ferguson A (2019) Thermal landscapes in a changing climate: biological implications of water temperature patterns in an extreme year. *Can J Fish Aquat Sci* 76(10):1740–1756. <https://doi.org/10.1139/cjfas-2018-0244>
- Stream-Solute-Workshop (1990) Concepts and methods for assessing solute dynamics in stream ecosystems. *J N Am Benthol Soc* 9:95–119
- Swanson FJ, Jones JA (2002) Geomorphology and hydrology of the HJ Andrews experimental forest, Blue River, Oregon. In: Field guide to geologic processes in Cascadia: field trips to accompany the 98th Annual Meeting of the Cordilleran Section of the Geological Society of America, May 13–15, 2002, Corvallis, Oregon. Oregon Department of Geology and Mineral Industries Portland, OR. pp 289–313
- Tank JL, Dodds WK (2003) Nutrient limitation of epilithic and epiphytic biofilms in ten North American streams. *Freshw Biol* 48(6):1031–1049. <https://doi.org/10.1046/j.1365-2427.2003.01067.x>
- Tank JL, Marti E, Riis T, von Schiller D, Reisinger AJ, Dodds WK, Whiles MR, Ashkenas LR, Bowden WB, Collins SM, Crenshaw CL, Crowl TA, Griffiths NA, Grimm NB, Hamilton SK, Johnson SL, McDowell WH, Norman BM, Rosi EJ, Simon KS, Thomas SA, Webster JR (2018) Partitioning assimilatory nitrogen uptake in streams: an analysis of stable isotope tracer additions across continents. *Ecol Monogr* 88(1):120–138. <https://doi.org/10.1002/ecm.1280>
- Van Loon AF, Gleeson T, Clark J, Van Dijk AIJM, Stahl K, Hannaford J, Di Baldassarre G, Teuling AJ, Tallaksen LM, Uijlenhoet R, Hannah DM, Sheffield J, Svoboda M, Verbeiren B, Wagener T, Rangelcroft S, Wanders N, Van Lanen HAJ (2016) Drought in the anthropocene. *Nat Geosci* 9(2):89–91
- VerHoef J, Peterson E, Clifford D, Shah R (2014) SSN: an R package for spatial statistical modeling on stream networks. *J Stat Softw* 56(3):45
- Ward AS, Wondzell SM, Schmadel NM, Herzog SP (2020) Climate change causes river network contraction and disconnection in the HJ Andrews Experimental Forest, Oregon, USA. *Front Water* 2:ARTN 7. <https://doi.org/10.3389/frwa.2020.00007>
- Warren DR, Collins SM, Purvis EM, Kaylor MJ, Bechtold HA (2017) Spatial variability in light yields colimitation of primary production by both light and nutrients in a forested stream ecosystem. *Ecosystems* 20(1):198–210. <https://doi.org/10.1007/s10021-016-0024-9>
- Wollheim WM, Bernal S, Burns DA, Czuba JA, Driscoll CT, Hansen AT, Hensley RT, Hosen JD, Inamdar S, Kaushal SS, Koenig LE, Lu YH, Marzadri A, Raymond PA, Scott D, Stewart RJ, Vidon PG, Wohl E (2018) River network saturation concept: factors influencing the balance of biogeochemical supply and demand of river networks. *Biogeochemistry* 141(3):503–521. <https://doi.org/10.1007/s10533-018-0488-0>
- Zimmer MA, Bailey SW, McGuire KJ, Bullen TD (2013) Fine scale variations of surface water chemistry in an ephemeral to perennial drainage network. *Hydrol Process* 27(24):3438–3451. <https://doi.org/10.1002/Hyp.9449>

Publisher's Note Springer Nature remains neutral with regard to jurisdictional claims in published maps and institutional affiliations.